



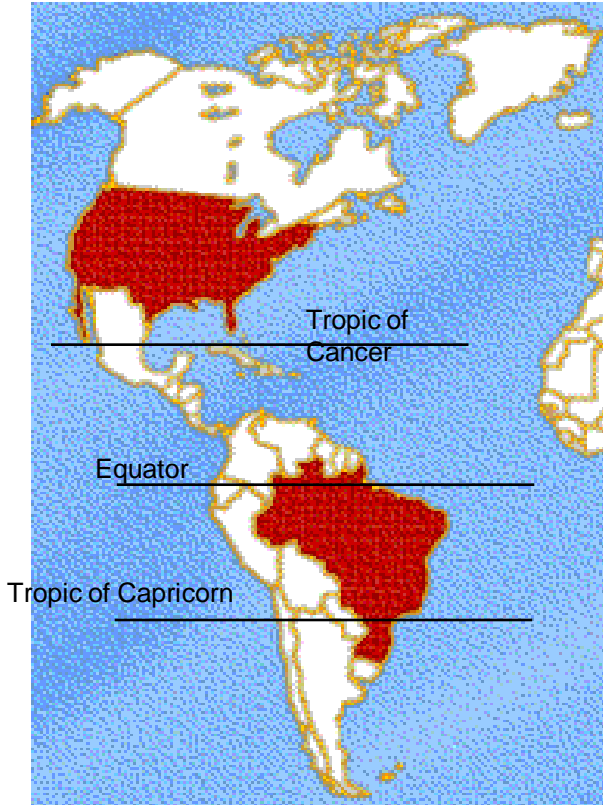
UNIVERSIDADE
FEDERAL DO CEARÁ

**POTENTIAL ADSORBENTS FOR
CHROMATOGRAPHY-BASED
PURIFICATION/SEPARATION PROCESSES OF
BIOMOLECULES**

Ivanildo J. Silva Jr. and Diana C. S. Azevedo

SAASA-2, San Luis, Feb 2013

Brasil



27 states

1 Federal District (Brasilia)

Population: 175million

Area: 8.5 million Km²

UNIVERSIDADE FEDERAL DO CEARÁ

(founded 1955)

GPSA - 18 ANOS

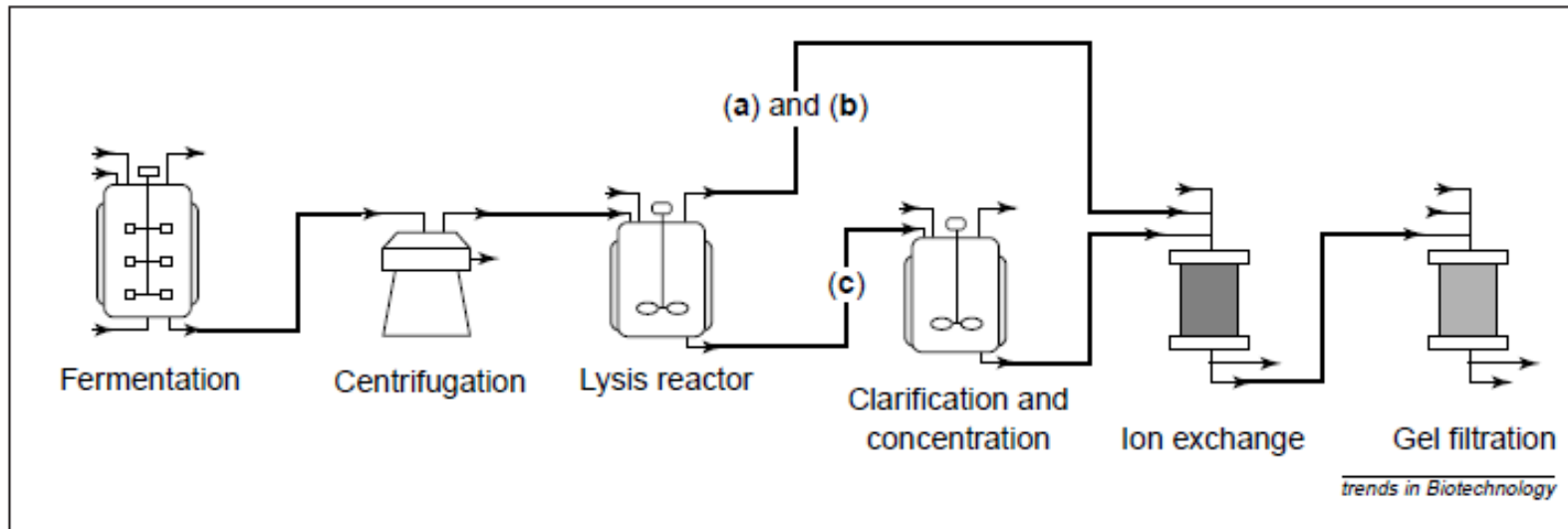
Fev/2013

LPACO2 - Laboratório de Pesquisa em
Adsorção e Captura de CO₂



Introduction

- General sequence of biomolecule production: upstream and downstream processing

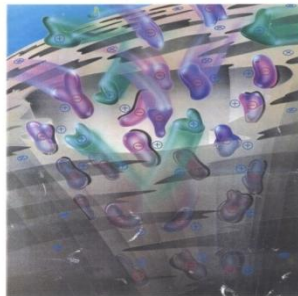


Downstream Processing

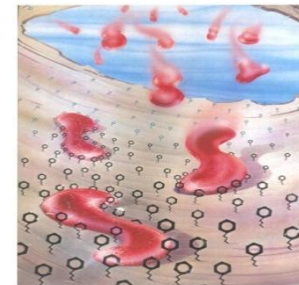
- high costs
- Long sequence of unit operations
- Challenge: productivity enhancement, reduction in operation time and costs

Introduction

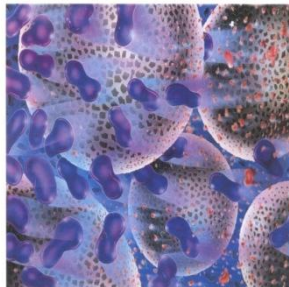
In chromatographic purification of proteins, ion exchange resins are the most common stationary phase, but hydrophobic interactions, gel filtration and affinity chromatography are also used in series.



Ion Exchange



Hydrophobic Interaction



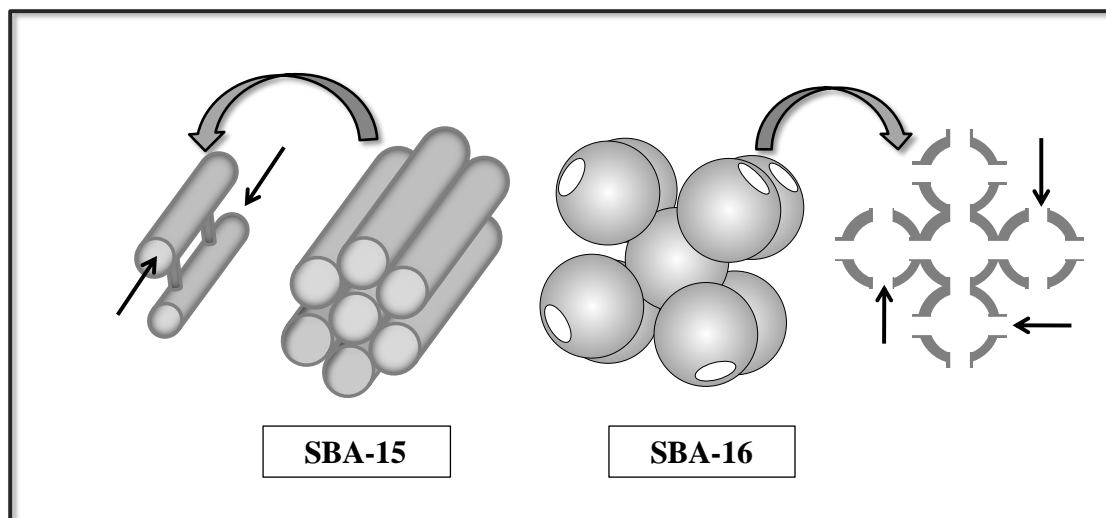
Size Exclusion



Affinity ligands

Introduction

In general, stationary phases for protein chromatography are based on styrene divinyl benzene copolymers with different degrees of crosslinking



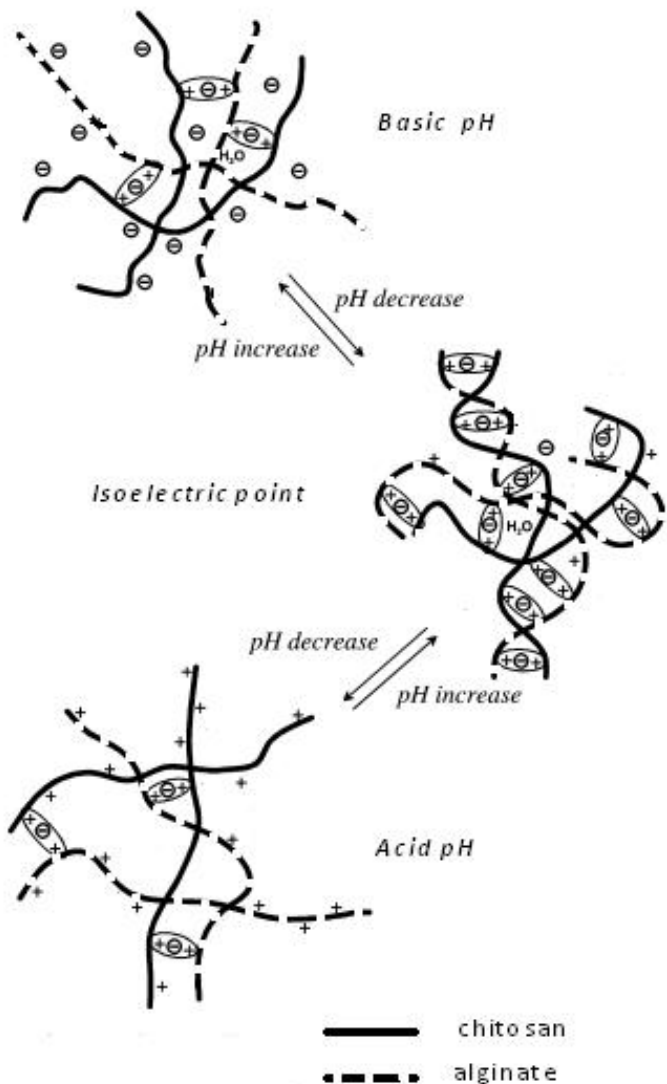
(I)

Zhao, D. et al. *JACS* **1998**, 120, 6024.

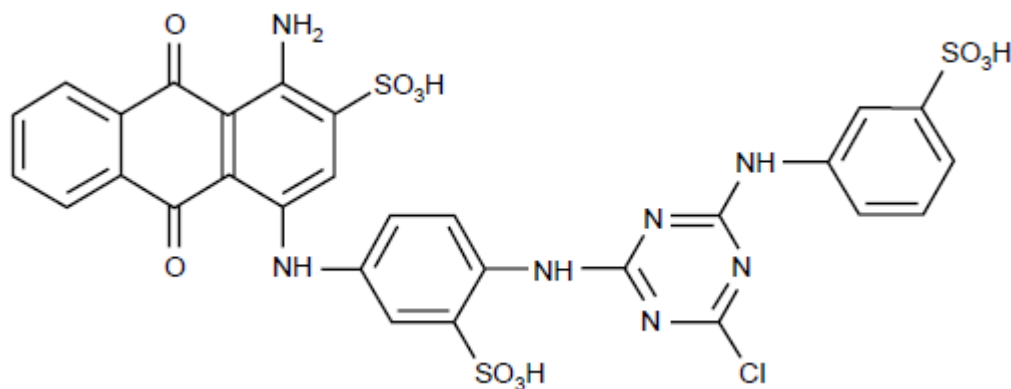
Flodström, K. et al.. *Langmuir* **2004**, 20,10311

large surface areas, well-defined pore structure, inert framework, nontoxicity, high biocompatibility, thermal and hydrothermal stability

Introduction



Chitosan-Alginate composites crosslinked with epichlorohydrin (Rodrigues et al., Ads Sci and Technol, 2012)



Cybacron Blue F3GA

Berger et al. **2004** *European Journal of Pharmaceutics and Biopharmaceutics*, 57,19.

(II)

Objective

Synthesize (I) nanostructured silicas and (II) dye-ligand chitosan/alginate composites and measure adsorption isotherms and column dynamics for the adsorption of model proteins (BSA, lysosime and IgG)

Experimental



- Characterization of adsorbents

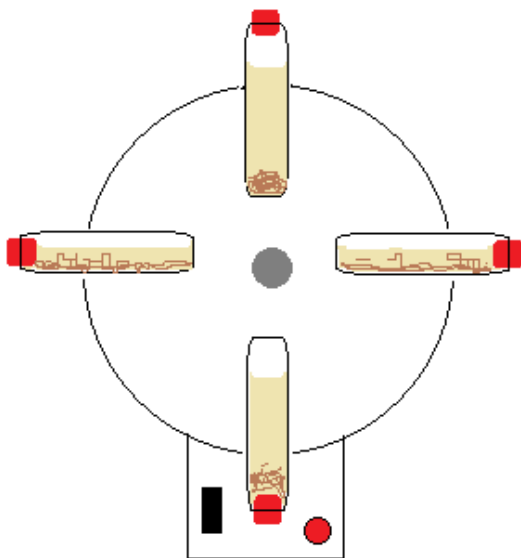
- ✓ Textural analysis (I);
- ✓ X-ray diffraction (I);
- ✓ TEM (Transmission Electron Microscopy) (I);
- ✓ XPS (X-ray Photoelectron Spectroscopy) (I).
- ✓ FTIR Spectroscopy (II)

- Adsorption tests

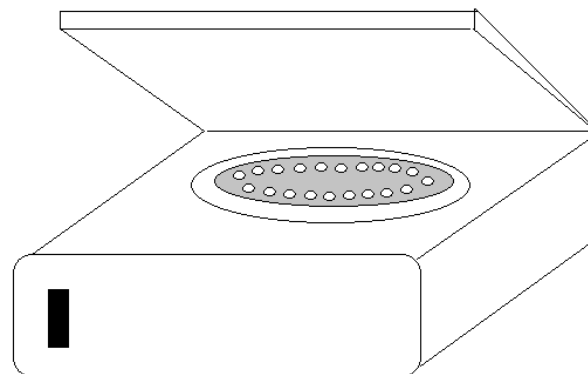
- ✓ Batch Kinetics of adsorption.
- ✓ Adsorption isotherms.
- ✓ Fixed bed operation.

Experimental (cont.)

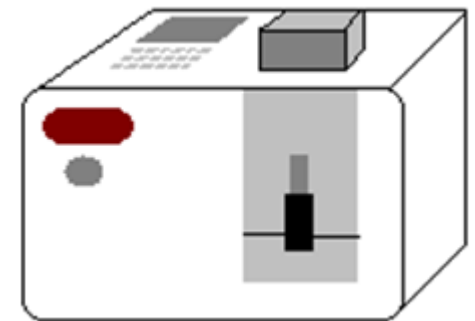
Batch adsorption



1



2



3

Figure 1 - Orbital shaker (1), refrigerated microcentrifuge (2) and spectrophotometer (5).

Experimental (Cont.)

Low-pressure chromatographic setup

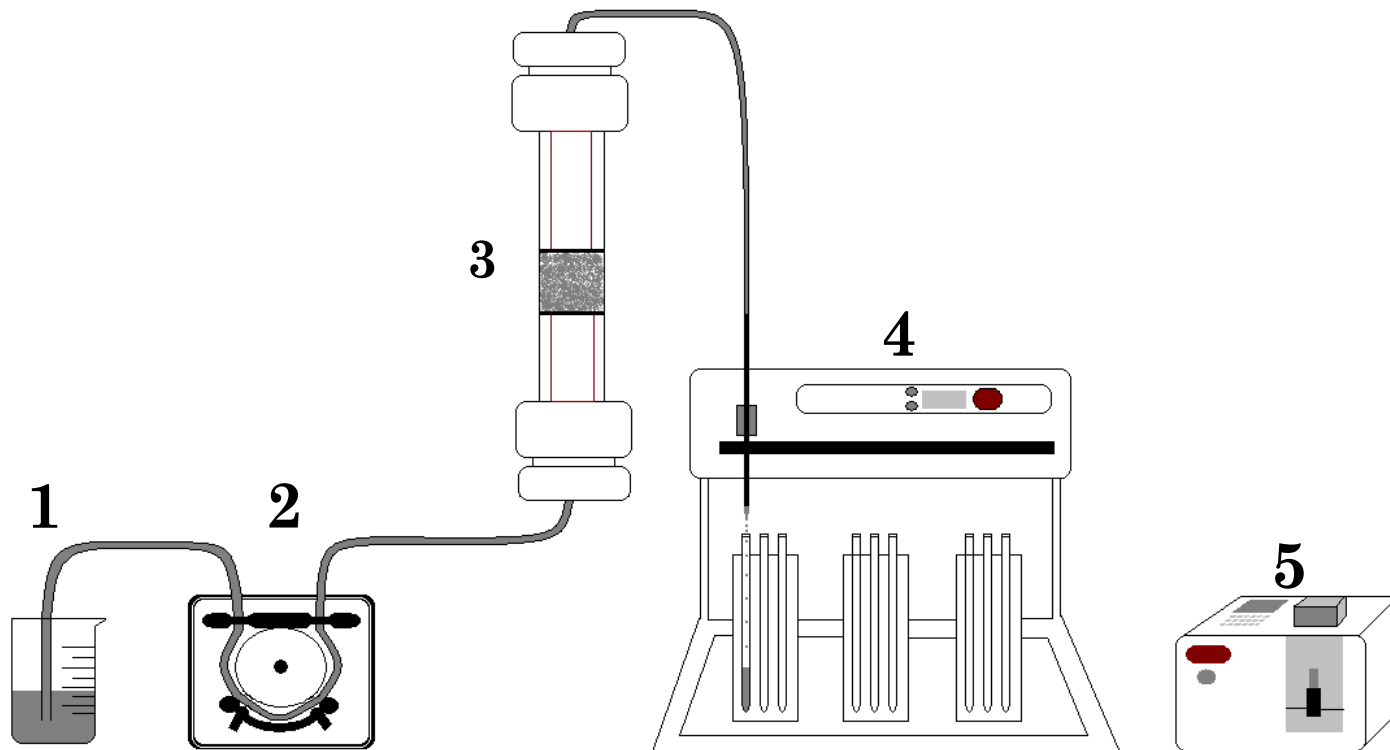


Figure 2 - Feed tank (1), peristaltic pump (2), chromatographic column (3), fraction collector (4) and spectrophotometer (5).

(I) Nanostructured silicas

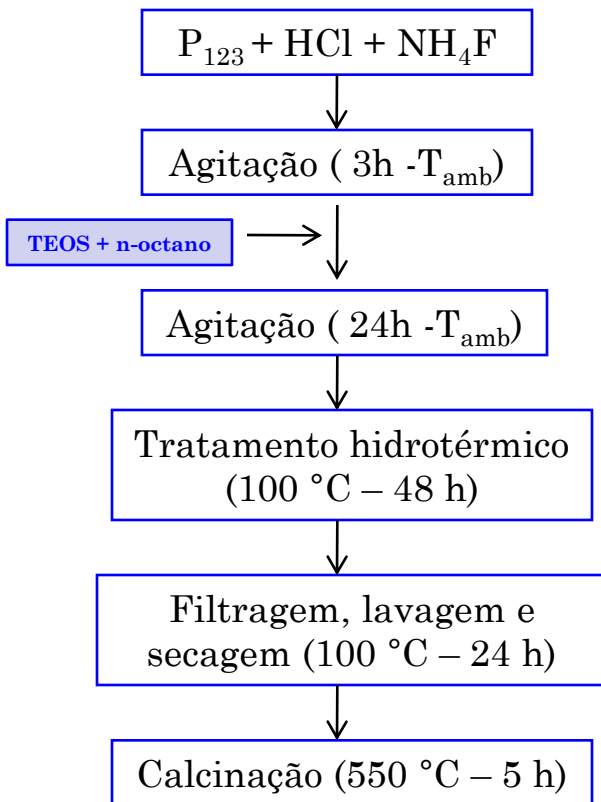


Synthesis and Characterization of Ordered Mesoporous Silica (SBA-15 and SBA-16) for Adsorption of Biomolecules

Experimental

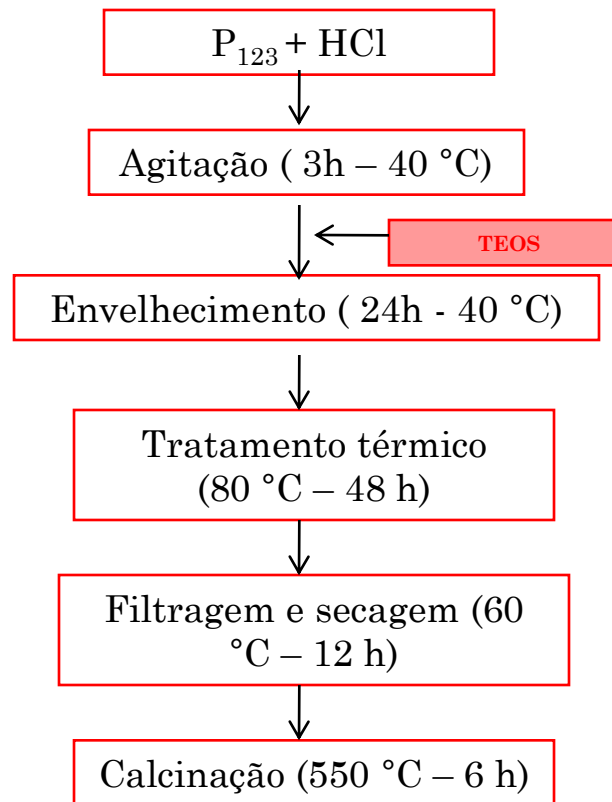
Síntese dos adsorventes

SBA-15 (hidrotérmico)



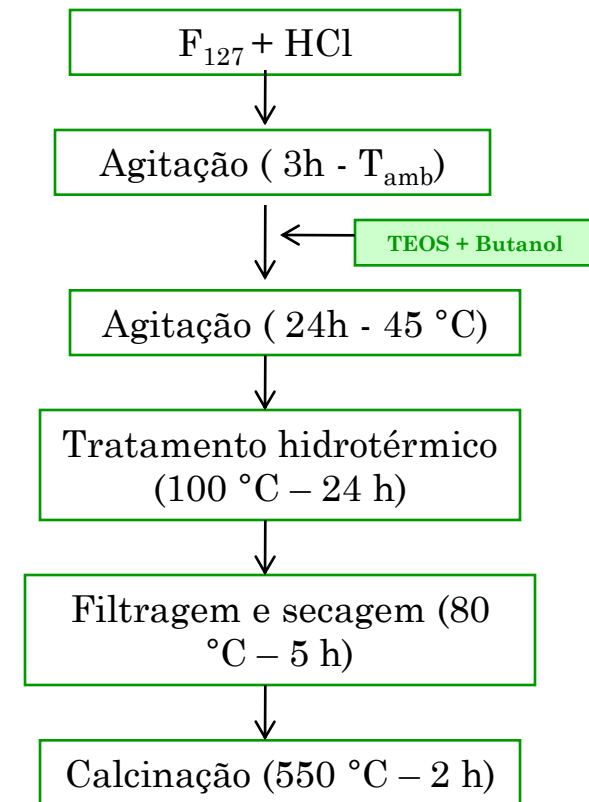
ZHANG *et al.* (2005)

SBA-15 (sol-gel)



ESPARZA *et al.* (2004)

SBA-16 (hidrotérmico)



RAFAL; BOGNA; MIETEK, (2006).

SBA-15 and SBA-16 for biomolecule adsorption - XRD results

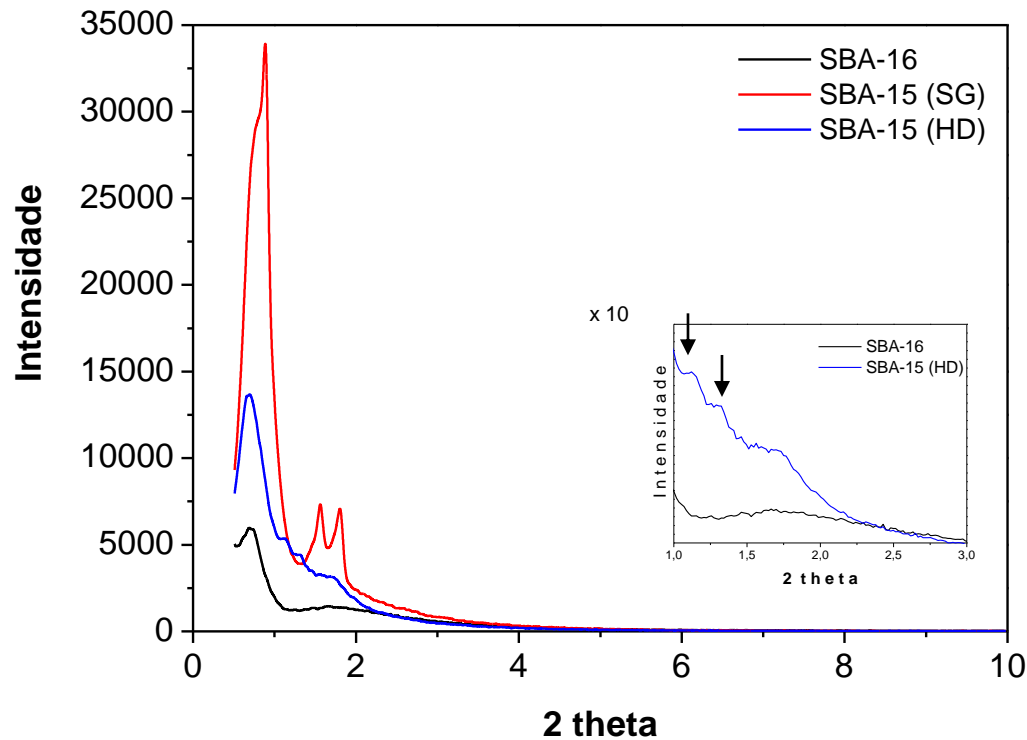


Figure 1.1 - X-ray diffraction of SBA-16, SBA-15 SG and SBA-15 HD samples.

SBA-15 and SBA-16 for biomolecule adsorption - TEM images

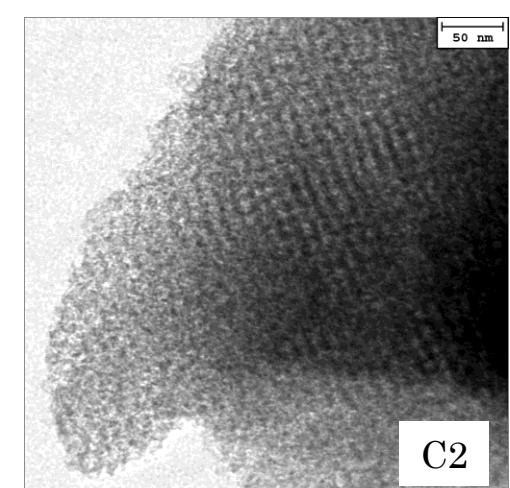
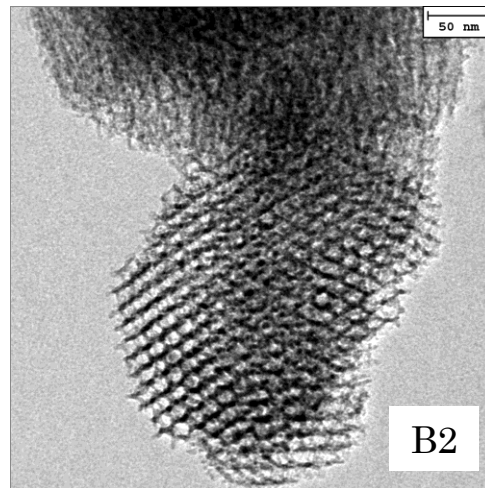
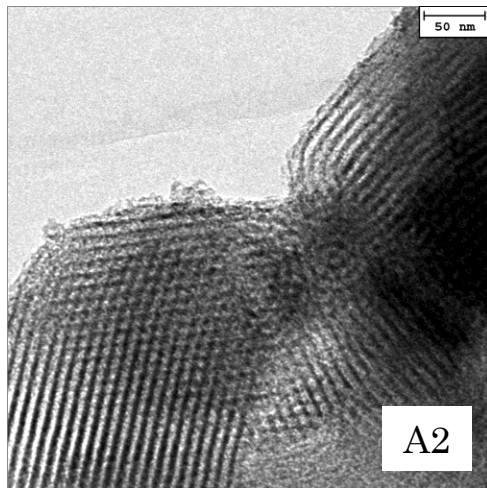
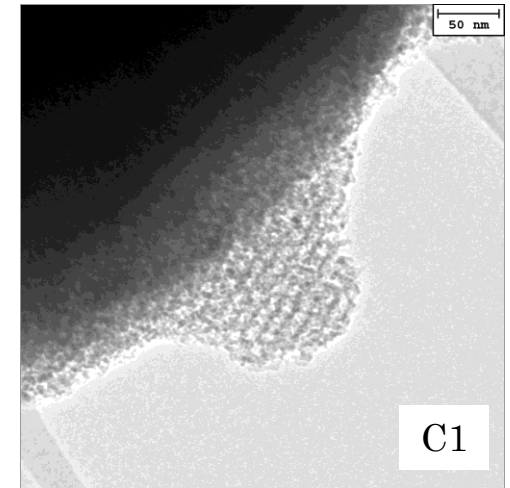
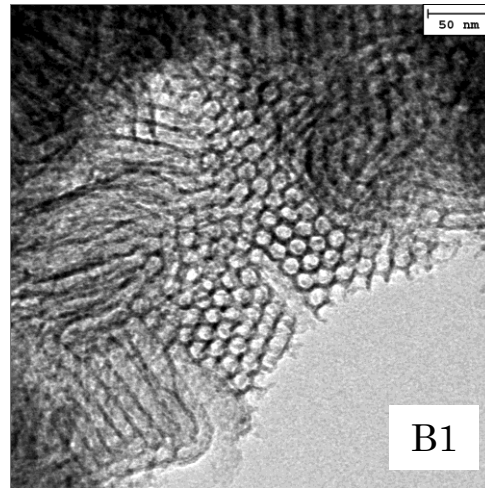
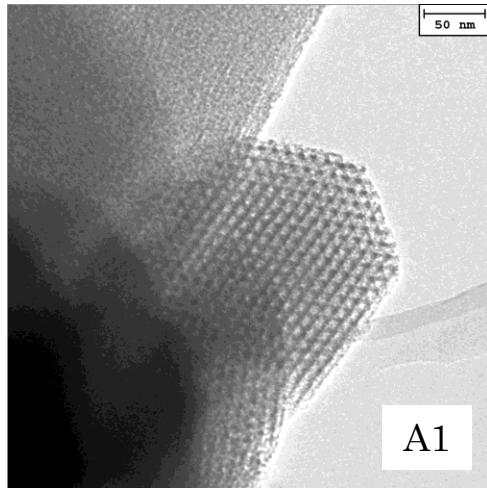


Figure 1.2 - TEM images of sample SBA-15 SG (A1 - A2), SBA-15 HD (B1 - B2) and SBA-16 (C1 - C2).

SBA-15 for biomolecule adsorption - N_2 adsorption/desorption isotherms

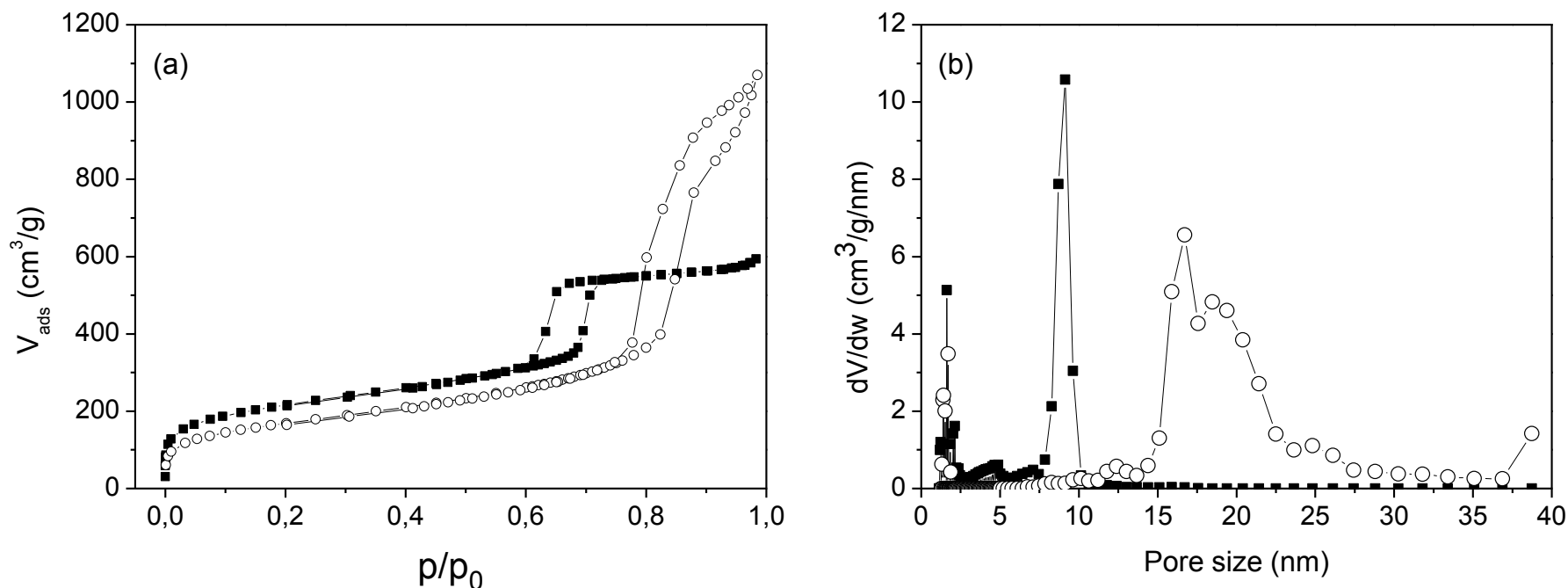


Figure 1.3 - Nitrogen adsorption isotherm (a) and NLDFT pore size distribution (b) for the SBA-15 SG (■) and SBA-15 HD (○).

SBA-16 for biomolecule adsorption - N_2 adsorption/desorption isotherms

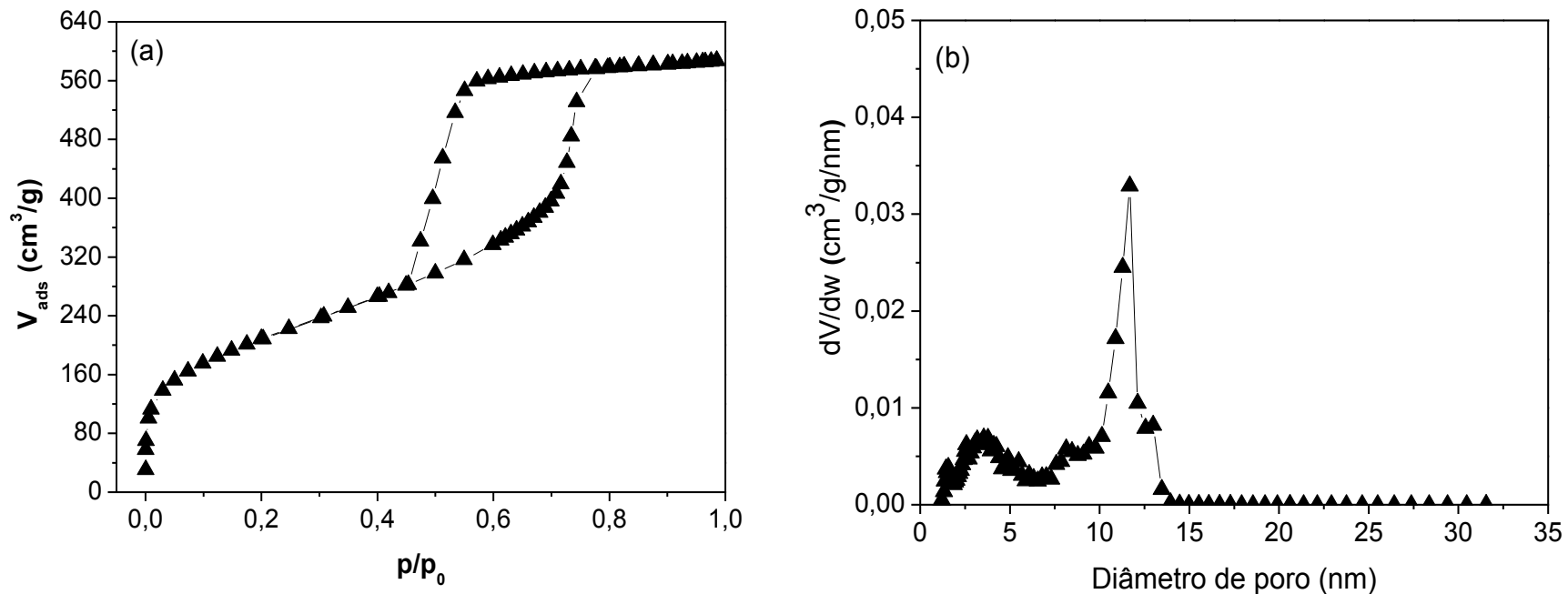


Figure 1.4 - Nitrogen adsorption isotherm (a) and NLDFT pore size distribution (b) for the SBA-16 (\blacktriangle).

SBA-15 and SBA-16 for biomolecule adsorption - Textural properties

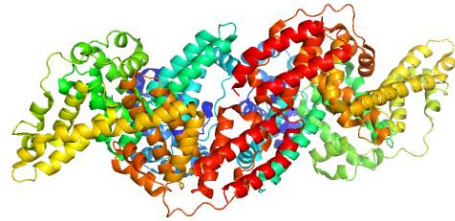


Table 1.1 - Textural properties of the SBA-15 HD, SBA-15 SG and SBA-16 samples.

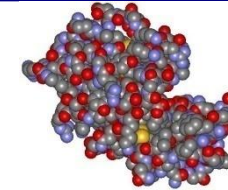
Samples	S_{BET} ($\text{m}^2 \cdot \text{g}^{-1}$)	Dp (nm)	V_p ($\text{cm}^3 \cdot \text{g}^{-1}$)
SBA-15 HD	609	16.7	1.65
SBA-15 SG	777	9.1	0.92
SBA-16	755	11.7	0.91

S_{BET} = surface area; Dp = pore diameter, obtained from the BJH method desorption branch; V_p = total pore.

SBA-15 and SBA-16 for biomolecule adsorption - uptake as function of pH



4 nm X 4 nm X 14 nm
pI = 4.8



3 nm X 3 nm X 4.5 nm
pI = 11.0

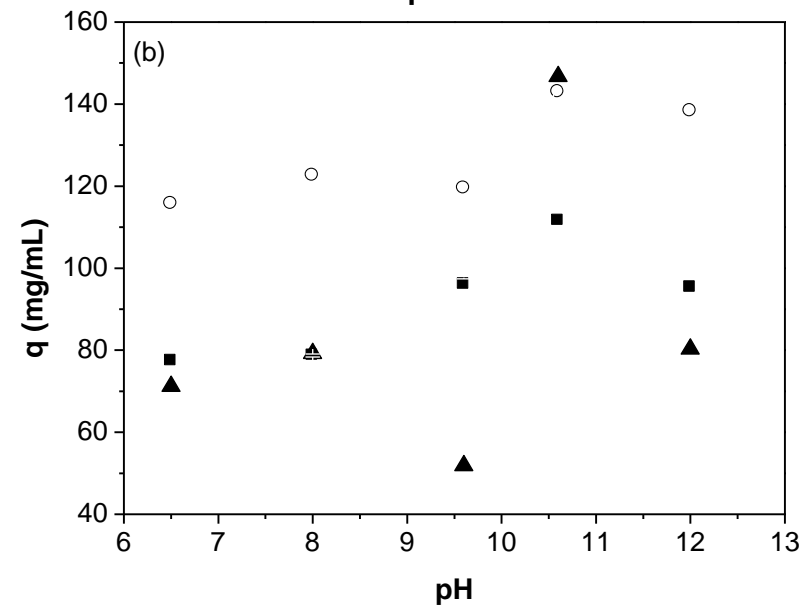
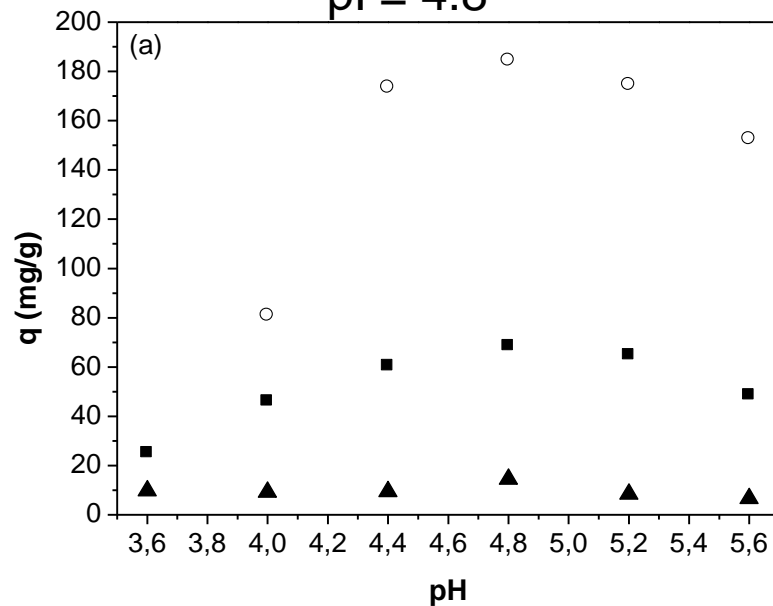
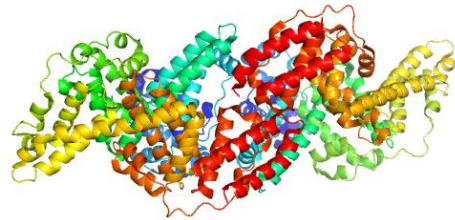
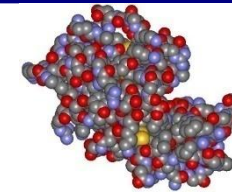
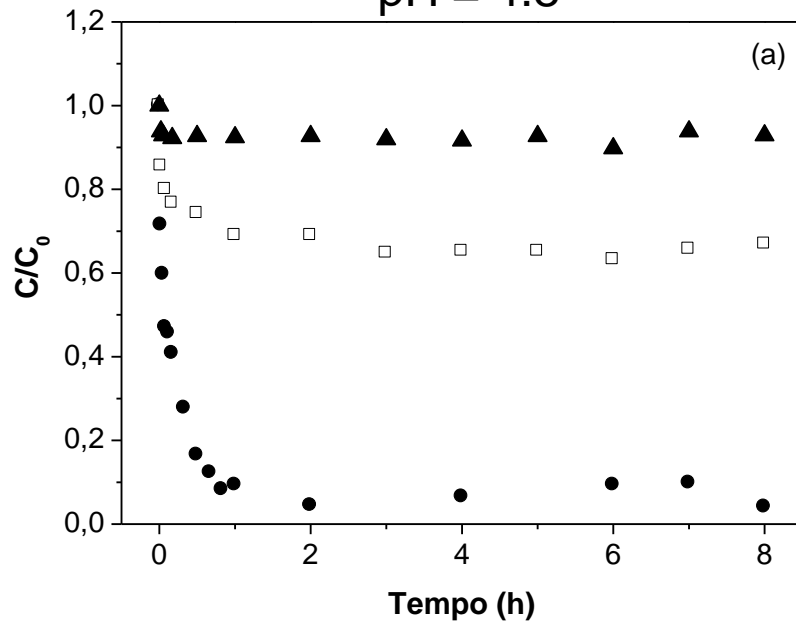


Figure 1.5 - Influence of pH on adsorption of BSA (a) and lysozyme (b) in SBA-15 obtained by sol-gel (■), hydrothermal (○) and SBA-16 (▲).

SBA-15 and SBA-16 for biomolecule adsorption - uptake rate at optimal pH



4 nm X 4 nm X 14 nm
pH = 4.8



3 nm X 3 nm X 4.5 nm
pH = 11.0

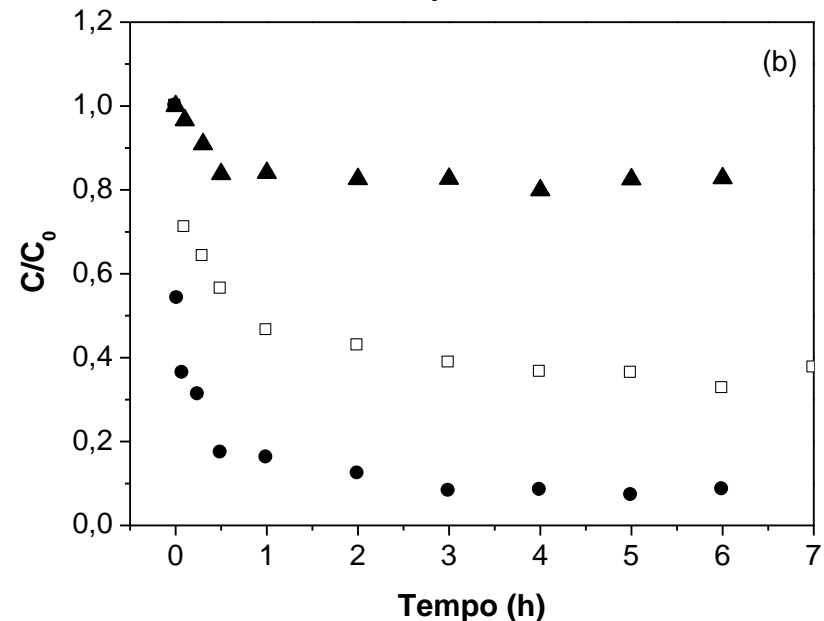


Figure 1.6 – Kinetic of adsorption of BSA (a) and lysozyme (b) in SBA-15 sol-gel (□), SBA-15 hydrothermal (●) and SBA-16 (▲).

SBA-15 and SBA-16 for biomolecule adsorption - BSA adsorption isotherms

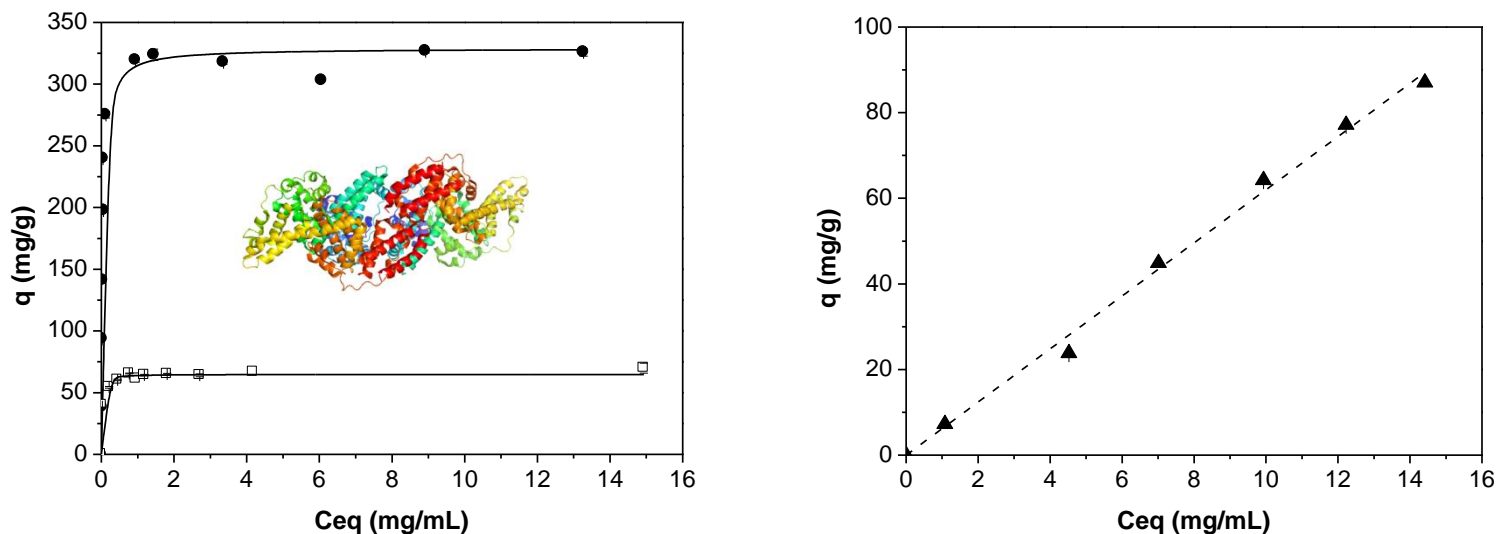


Figure 1.8 - BSA adsorption isotherms in SBA-15 sol-gel (\square), SBA-15 hydrothermal (\bullet) and SBA-16 (\blacktriangle). (—) Langmuir model; (--) Henry Model.

Table 1.2 - Parameters of the Langmuir equation for adsorption of BSA in mesoporous silica.

Sample	Model	Parameters			R^2
		$q_{\text{máx}}(\text{mg}\cdot\text{g}^{-1})$	b	k_H	
SBA-15 sol-gel	Langmuir	$65.02 \pm 1,35$	$70.52 \pm 17,62$	-	0.9682
SBA-15 hidrotermal	Langmuir	$328.74 \pm 14,86$	$23.10 \pm 4,98$	-	0.9195
SBA-16	Henry	-	-	$6.20 \pm 0,10$	0.9951

SBA-15 and SBA-16 for biomolecule adsorption - LYS adsorption isotherms

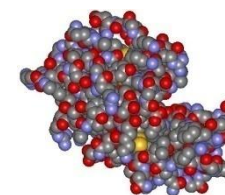
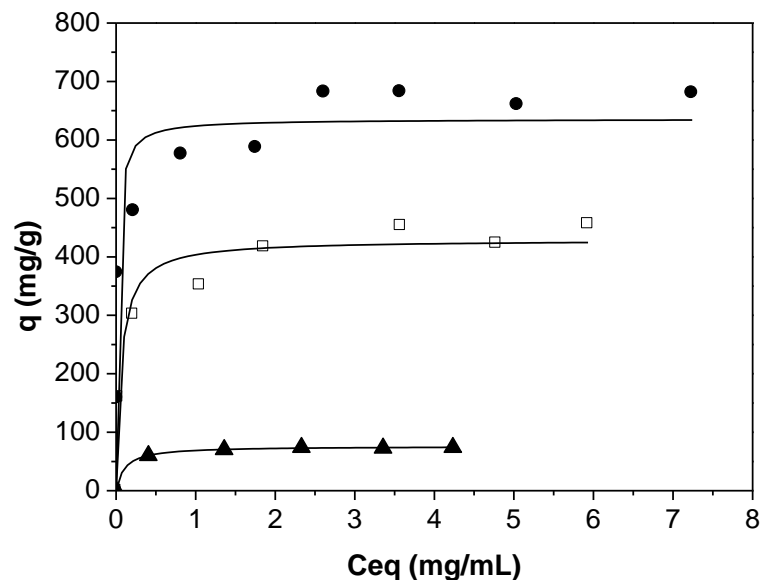


Figure 1.9 - Lysozyme adsorption isotherms in SBA-15 sol-gel (□), SBA-15 hydrothermal (●) and SBA-16 (▲). (—) Langmuir model.

Table 1.3 - Parameters of the Langmuir equation for adsorption of LYS in mesoporous silica.

Sample	Model	Parameters		R ²
		$q_{\text{máx}}(\text{mg}\cdot\text{g}^{-1})$	b	
SBA-15 sol-gel	Langmuir	429.10 ± 16.69	15.79 ± 5.12	0.9627
SBA-15 hydrothermal	Langmuir	635.69 ± 29.99	52.71 ± 19.17	0.9129
SBA-16	Henry	76.07 ± 0.58	9.35 ± 0.79	0.9994

SBA-15 for biomolecule adsorption - effect of changing pore width and length



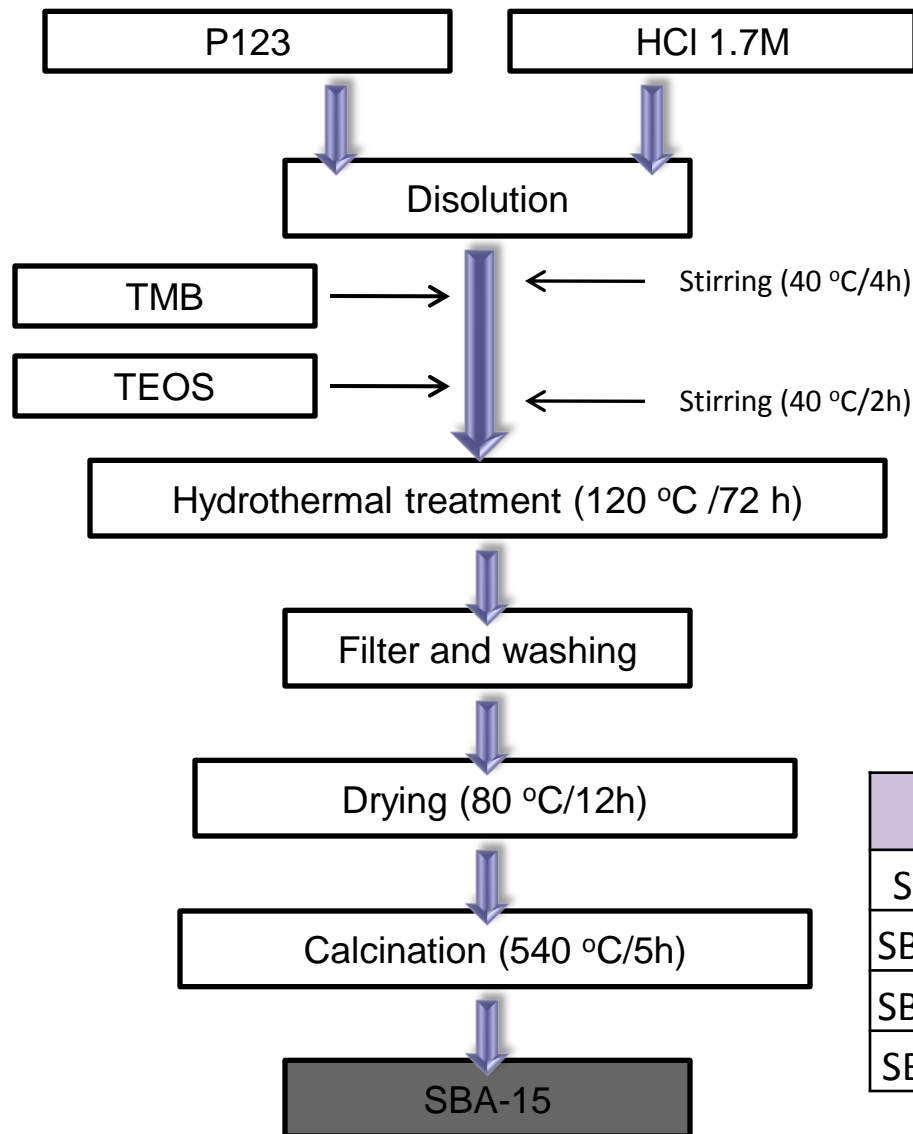
Swelling agent: 1,3,5-trimethylbenzene (TMB)

Attempts to shorten pore length

by the addition of

heptane and ammonium fluoride (NH_4F).

Experimental



Adapted from:

Fulvio et al, Journal of Materials Chemistry, 15 (2005) 5049.

Zhang et al., The Journal of Physical Chemistry B, 110 (2006) 25908

Table 1 – Synthesized materials.

Samples	
SBA-15 (S)	P123 + TEOS
SBA -15 (S1)	P123 + TMB +TEOS
SBA -15 (S2)	(P123 + NH ₄ F) + (HEPTANE + TEOS)
SBA-15 (S3)	(P123 + NH ₄ F) + TMB + TEOS

SBA-15 for biomolecule adsorption - Changing pore width and length

Results

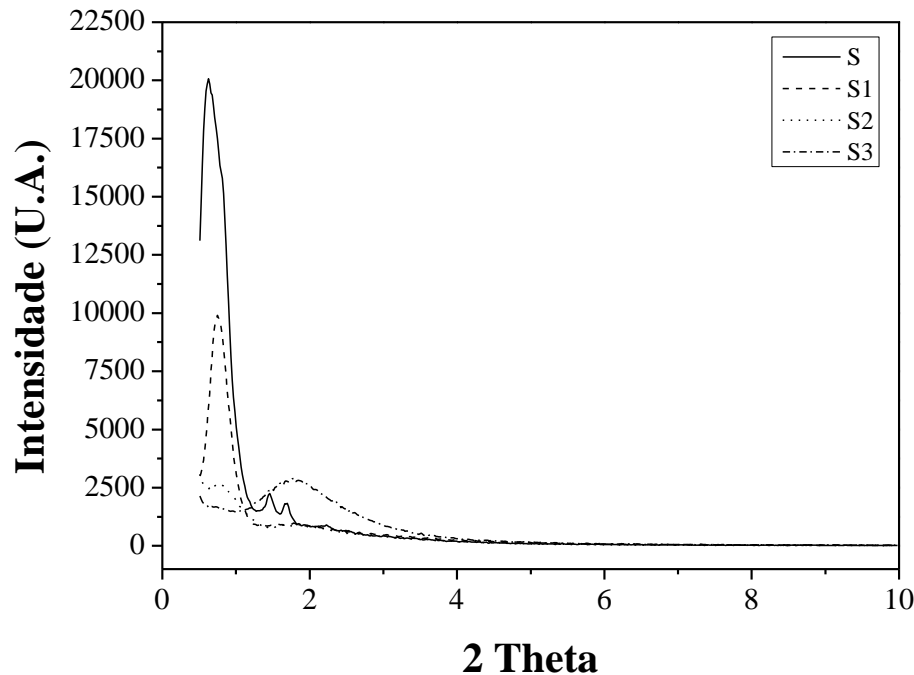


Figure 2.1 - XRD pattern of SBA-15 synthesized with and without swelling agent and calcined at 550 °C.

SBA-15 for biomolecule adsorption - Changing pore width and length

Results

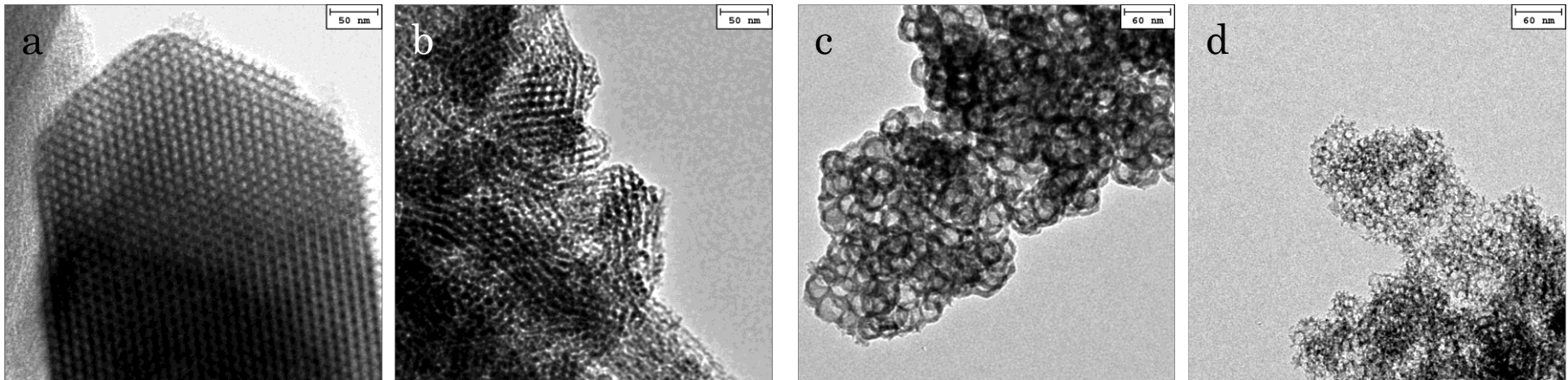


Figure 2.2 - TEM images of SBA-15 synthesized (a) S, (b) S1, (c) S2 and (d) S3.

SBA-15 for biomolecule adsorption - Changing pore width and length



Results

Table 2.1 - Adsorption and structural parameters for the SBA-15 samples studied.

Sample	S_{BET} ($\text{m}^2.\text{g}^{-1}$)	D_p (nm)	V_{TP} ($\text{cm}^3.\text{g}^{-1}$)
SBA-15	730	5.6	1.29
SBA-15/TMB	679	10.6	2.31
SBA-15/TMB_NH ₄ F	460	18.1	1.24
SBA-15/NH ₄ F_heptane	480	13.17	2.19
Hydrothermal SBA-15	609	16.7	1.65

SBA-15 for biomolecule adsorption - Changing pore width and length

Results - BSA

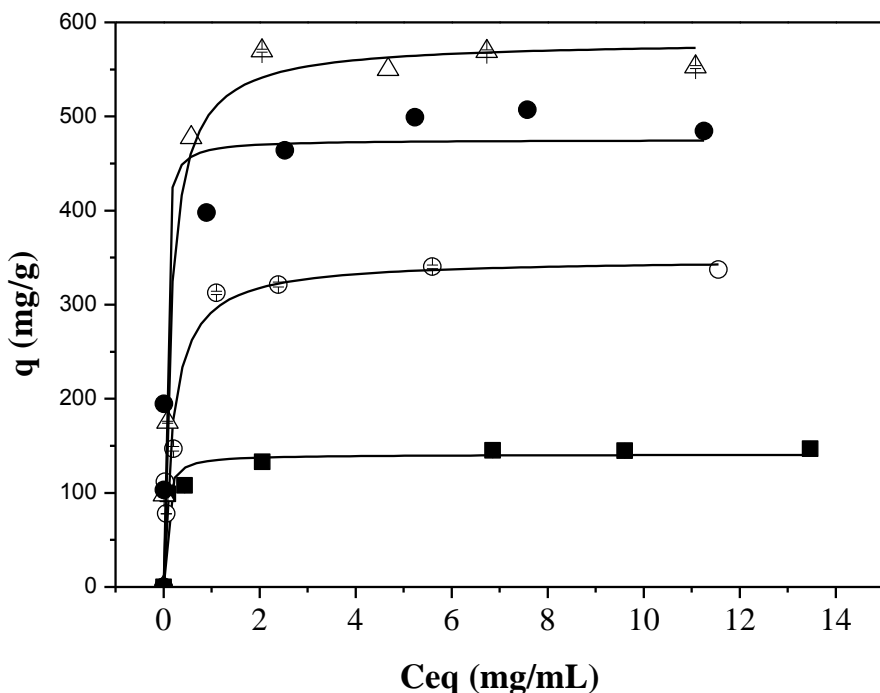


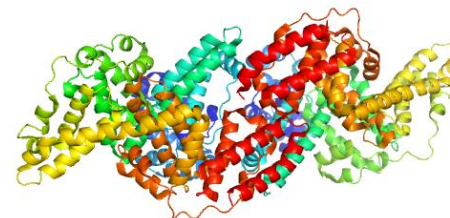
Figure 2.7 – Adsorption isotherms of BSA onto adsorbents (■) S, (○) S1, (△) S2 and (●) S3. (-) Langmuir Model. (25 °C, Buffer acetate pH = 4.8, t = 24 h).

Table 2.3 – Parameters of the Langmuir equation for adsorption BSA in mesoporous silica.

SBA-15	Parâmetros		R ²
	q _{máx} (mg.g ⁻¹)	b	
S	140.8 ± 5.1	20.5 ± 6.9	0,9682
S1	348.4 ± 19.3	5.2 ± 1.6	0,9562
S2	580.5 ± 18.1	6.8 ± 1.5	0,9843
S3	475.3 ± 19.1	44.0 ± 13.3	0,9633

SBA-15 328.74 23.10

S = SBA-15; S1 = SBA-15/TMB; S2 = SBA-15/TMB_NH₄F and S3 = SBA-15/NH₄F_heptane.



SBA-15 for biomolecule adsorption - Changing pore width and length

Results - LYS

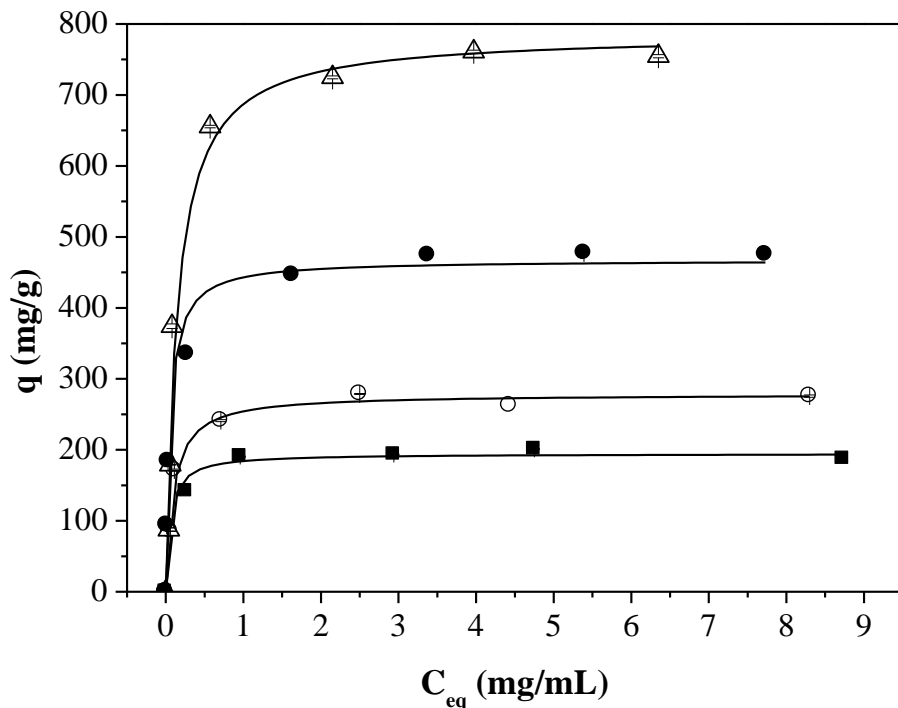


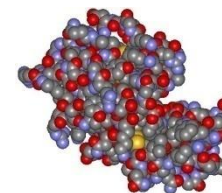
Figure 2.8 – Adsorption isotherms of LYS onto adsorbents (■) S, (○) S1, (Δ) S2 and (●) S3. (-) Langmuir Model. (25 °C, Buffer bicarbonate, pH = 10.6, t = 6h).

Table 2.4 – Parameters of the Langmuir equation for adsorption LYS in mesoporous silica.

SBA-15	Langmuir constants		R ²
	$q_{\text{máx}}$ (mg·g ⁻¹)	b	
S	195.5 ± 5.7	17.8 ± 3.9	0,9826
S1	278.5 ± 9.1	10.5 ± 1.9	0,9827
S2	786.0 ± 1,9	6.9 ± 1.5	0,9728
S3	467.0 ± 13.6	18.2 ± 3.8	0,9837

SBA-15 635.69 52.71

S = SBA-15; S1 = SBA-15/TMB; S2 = SBA-15/TMB_NH₄F and S3 = SBA-15/NH₄F_heptane.



SBA-15 for biomolecule adsorption - Changing pore width and length



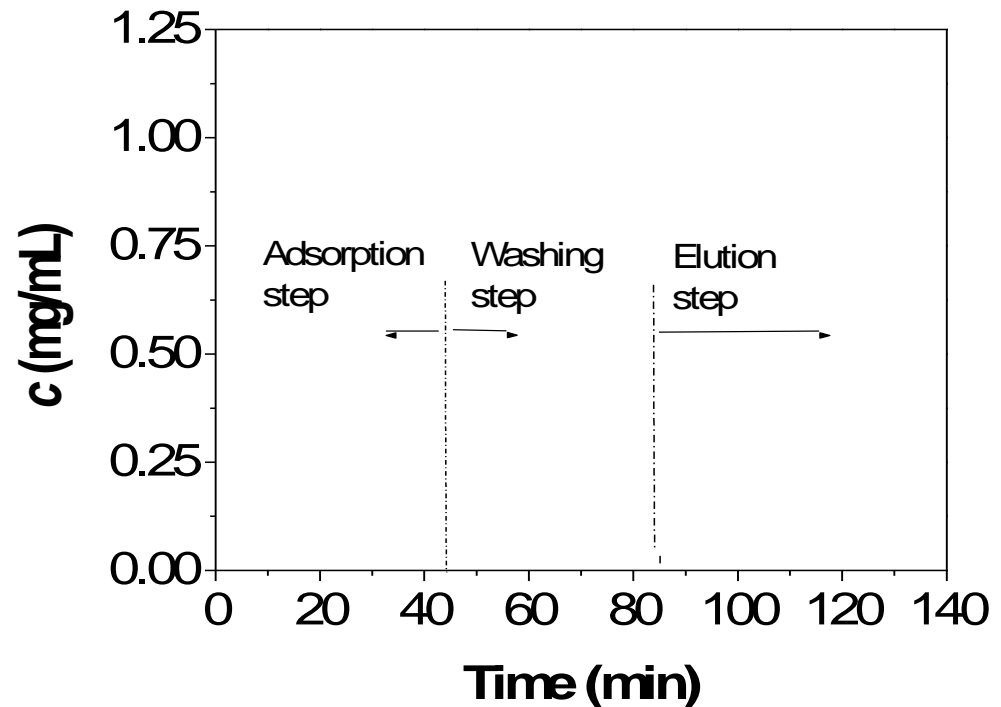
Summary

- The addition of TMB does contribute to pore expansion, nevertheless materials with similar porous texture may be obtained in the absence of TMB under proper hydrothermal synthesis conditions
- NH_4F and heptane tend to lead to very disordered materials, apparently with shorter pore lengths. Despite the significantly lower surface areas, the material prepared with TMB and NH_4F has considerably higher maximum capacities and a less rectangular isotherm, which may be interesting features for chromatographic separations

What about surface functionalities?

Background

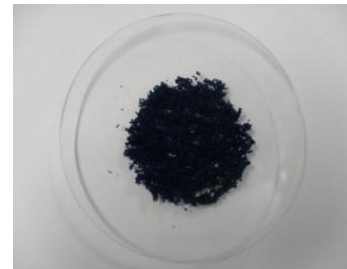
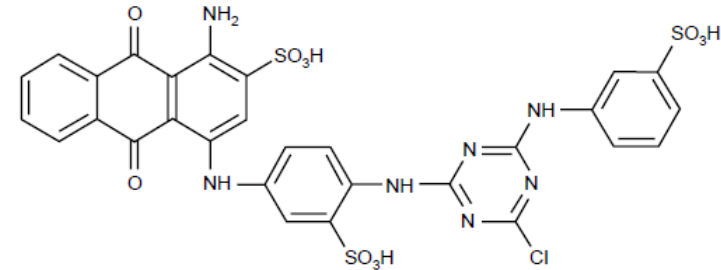
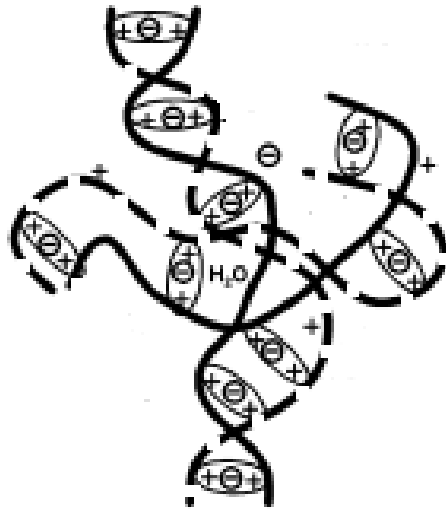
Epoxilated chitosan-alginate composite for cellulase adsorption



Rodrigues et al., Ads Sci & Technol, 2012

What about surface functionalities?

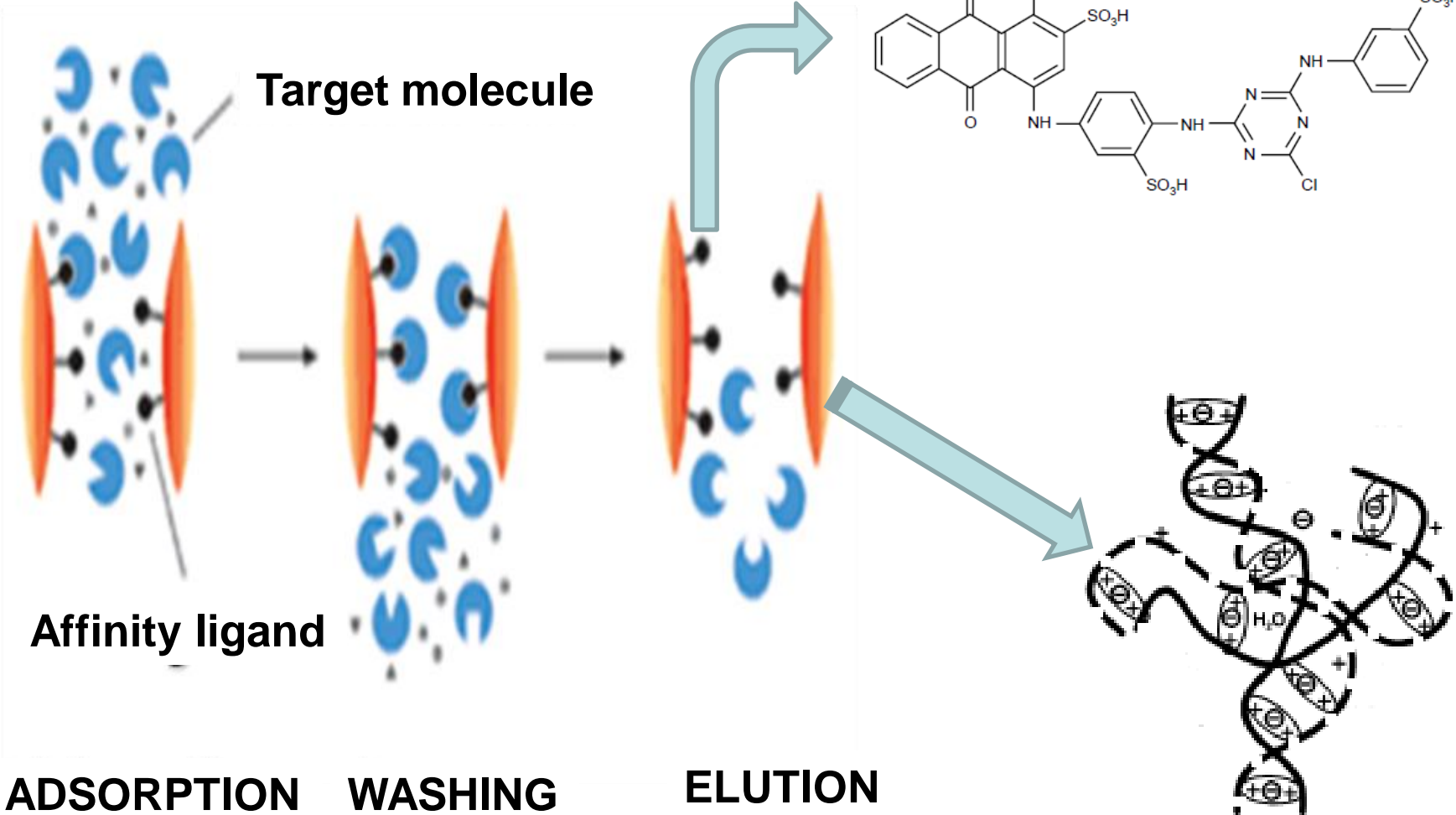
Isoelectric point



Gondim et al., Ads Sci & Technol,
30, 701-711, 2012

The objective of this work was to study a novel dye-ligand affinity adsorbent using the biopolymers chitosan and alginate with immobilized dyes (Cibacron Blue).

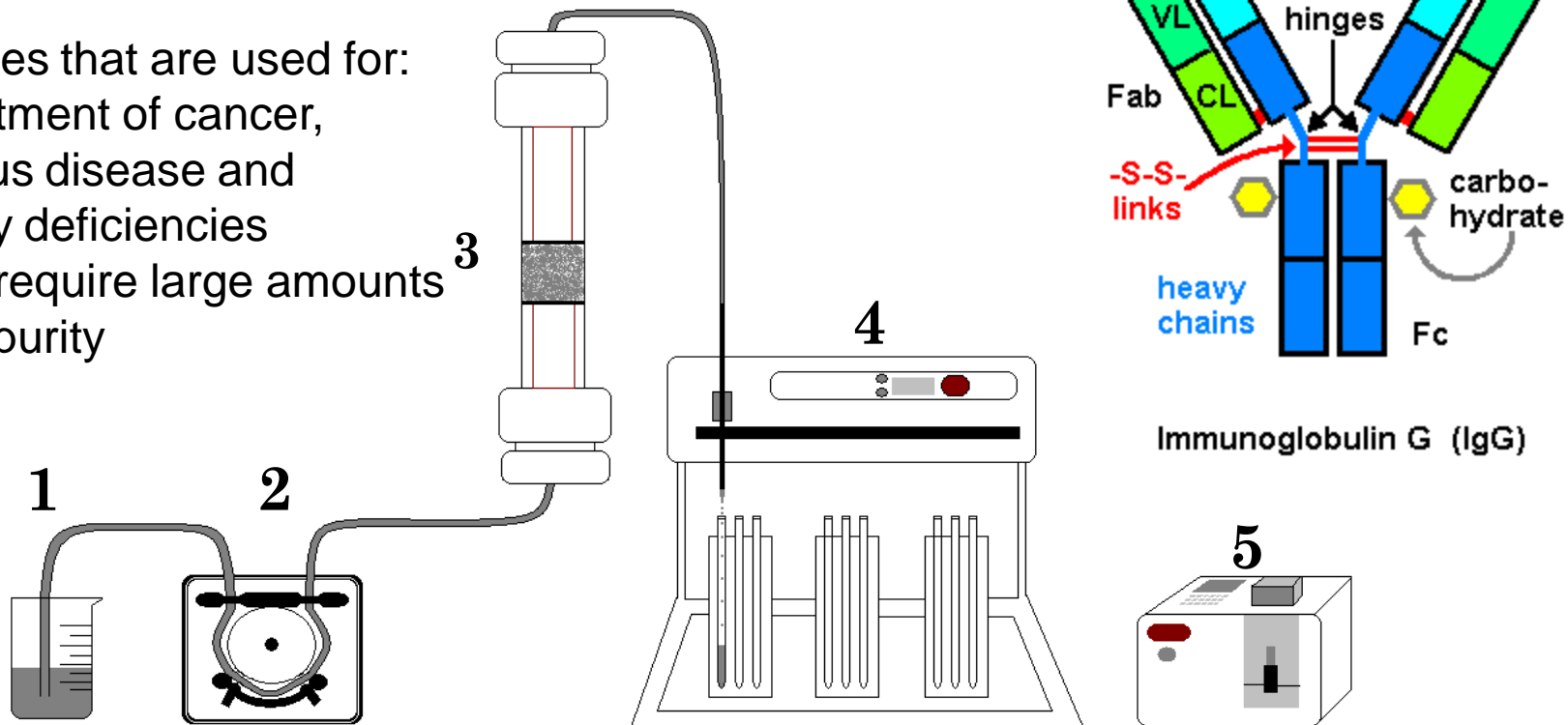
Principle of affinity chromatography



Experimental

- Target protein
Human IgG

antibodies that are used for:
the treatment of cancer,
infectious disease and
antibody deficiencies
usually require large amounts
of high-purity



Feed tank (1), peristaltic pump (2), chromatographic column (3), fraction collector (4) and spectrophotometer (5).

Adsorption of IgG in Dye-ligand E-Ch/Al

Uptake as a function of pH

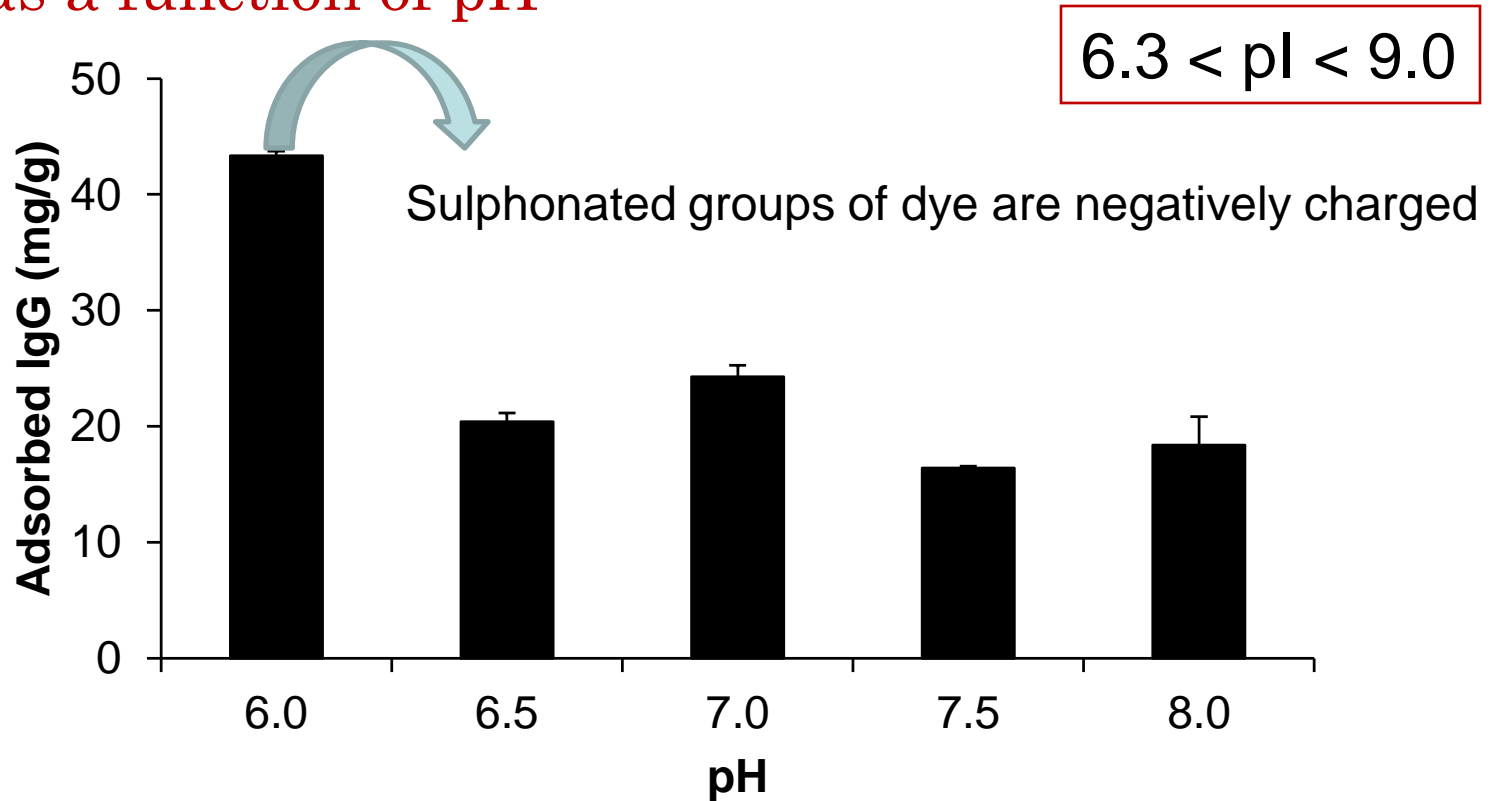


Figure 3.2. Effect of pH on IgG adsorption with Cibacron Blue Immobilized into epoxide chitosan/alginate. Adsorption buffer used: 25 mmol/L of sodium phosphate.

Adsorption of IgG in Dye-ligand E-Ch/Al

Batch adsorption kinetics

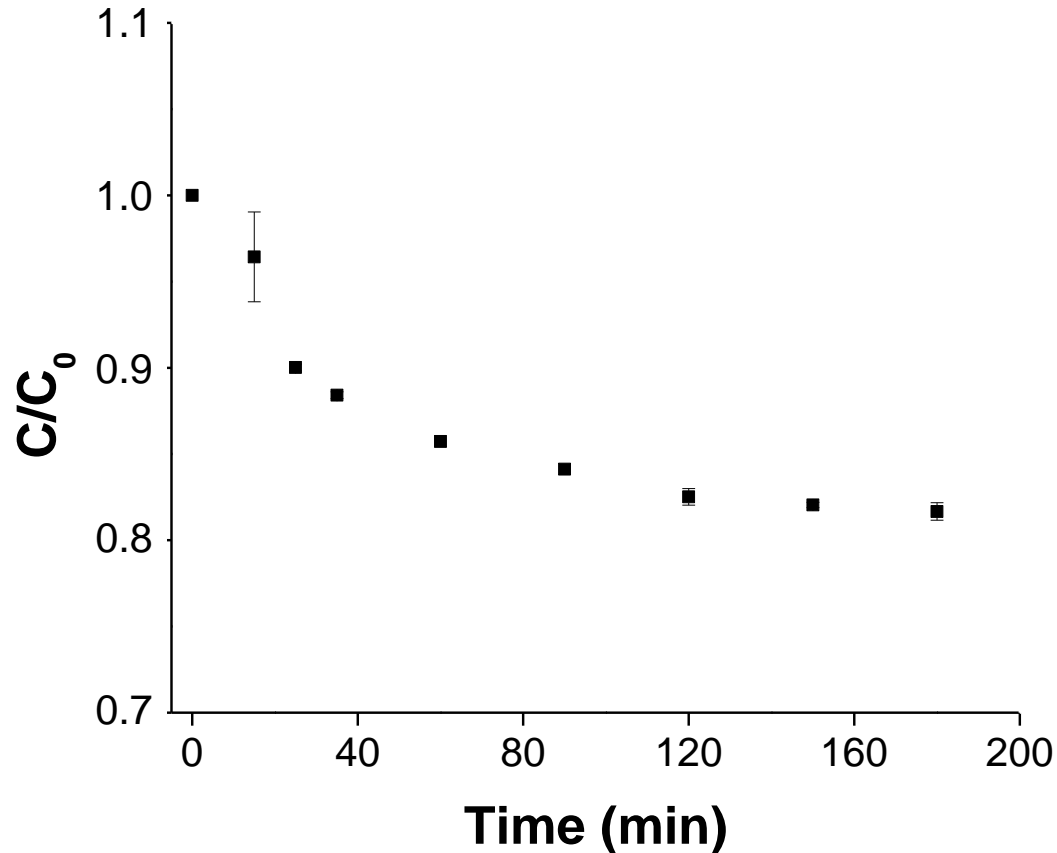


Figure 3.3. Kinetic profile for IgG adsorption with Cibacron Blue F3GA Immobilized into epoxide chitosan/alginate. Adsorption buffer used: 25 mmol/L of sodium phosphate.

Adsorption isotherm

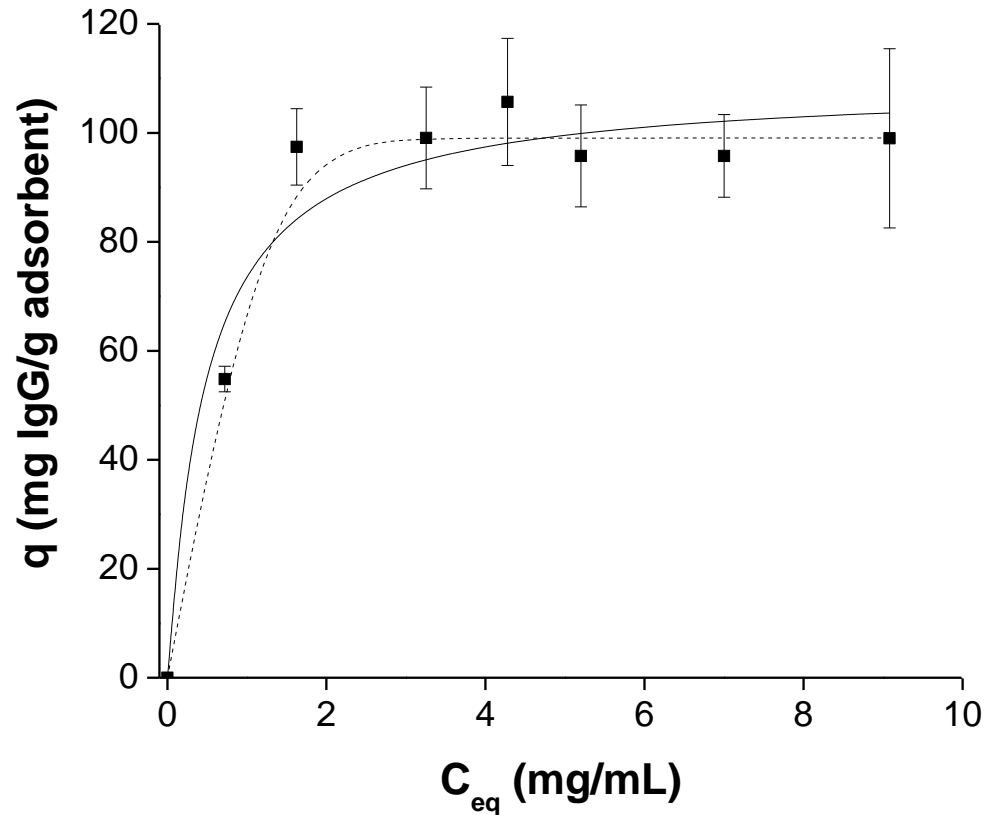


Figure 3.4. Adsorption isotherm of IgG on Cibacron Blue F3GA immobilized on E-Ch/Al. Theoretical profile: the solid and dashed lines correspond to fitting (nonlinear regression) of experimental data according to the Langmuir and Langmuir-Freundlich models, respectively.

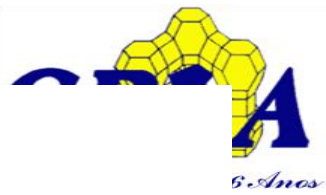
Adsorption of IgG in Dye-ligand E-Ch/Al



Adsorption isotherm parameters for diff buffers

Parâmetros	Cibacron Blue (FS 25mM)		Cibacron Blue (MOPS 25mM)		Cibacron Blue (HEPES 25mM)	
	Langmuir	Langmuir- Freundlich	Langmuir	Langmuir- Freundlich	Langmuir	Langmuir- Freundlich
q_m (mg/g)	$109.2 \pm 6,3$	$99,1 \pm 1,6$	$105,9 \pm 6,4$	$114,3 \pm 32,0$	$92,3 \pm 9,0$	$85,4 \pm 15,0$
K_D ($\times 10^6 M$)	$3,20 \pm 1,2$	-	$7,48 \pm 1,65$	-	$6,92 \pm 2,59$	-
K_{DLF} ($\times 10^6 M$)	-	$1,2 \pm 0,7$	-	$8,47 \pm 4,35$	-	$5,88 \pm 2,95$
n	-	$4,86 \pm 3,29$	-	$0,84 \pm 0,42$	-	$1,22 \pm 0,63$
R^2	0,952	0,993	0,965	0,966	0,912	0,913
χ^2	73,45	13,13	37,53	42,60	72,17	81,59

Adsorption of IgG in Dye-ligand E-Ch/Al



Fixed

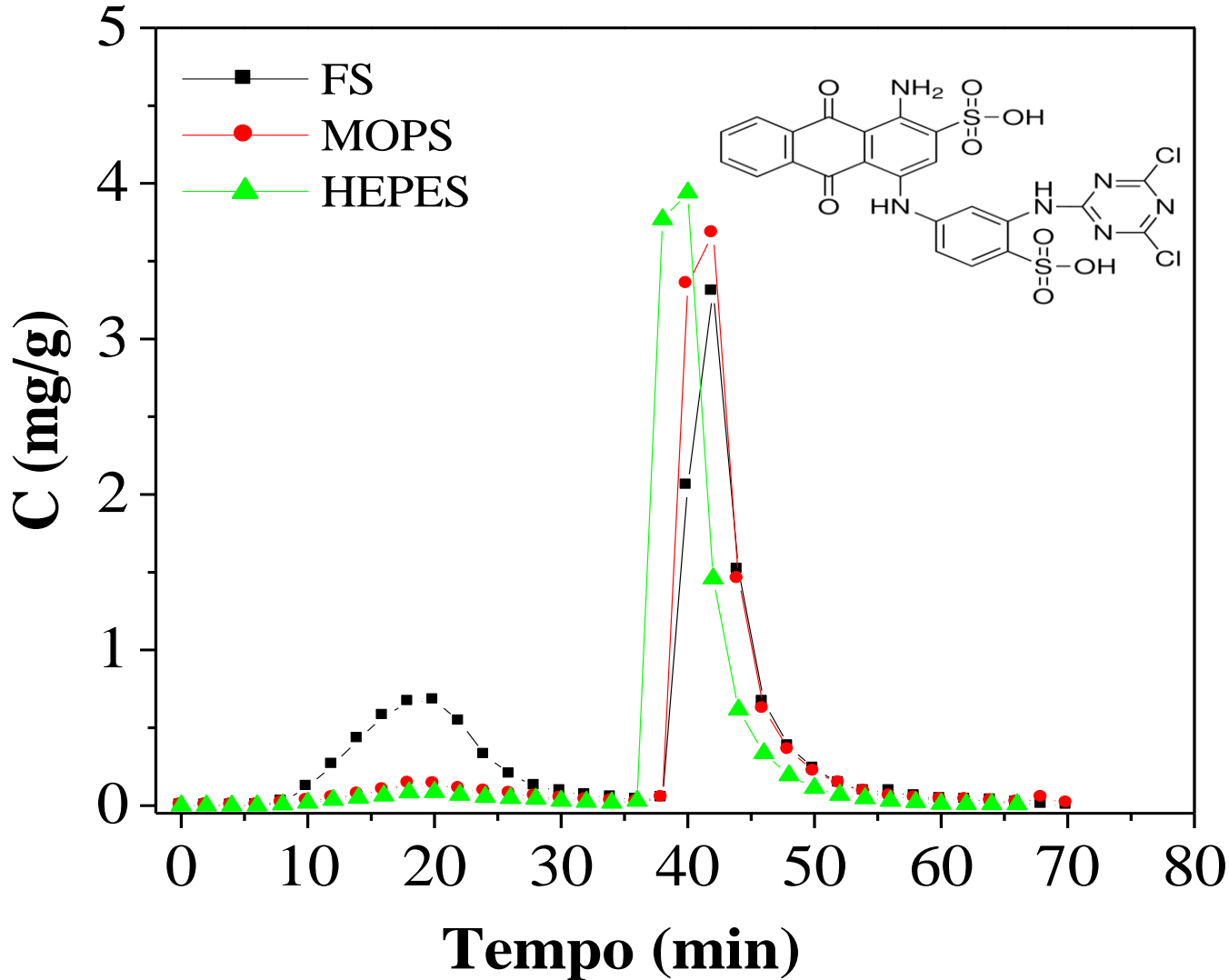


Figure showing the adsorption of IgG in dye-ligand E-Ch/Al immobilized on a support. The adsorption was performed in 25 mM phosphate buffer (pH 7.4) containing 50 mM of NaOH.

ure
3A
25
im
50

Adsorption of IgG in Dye-ligand E-Ch/Al

Fixed bed experiment w/ human blood serum

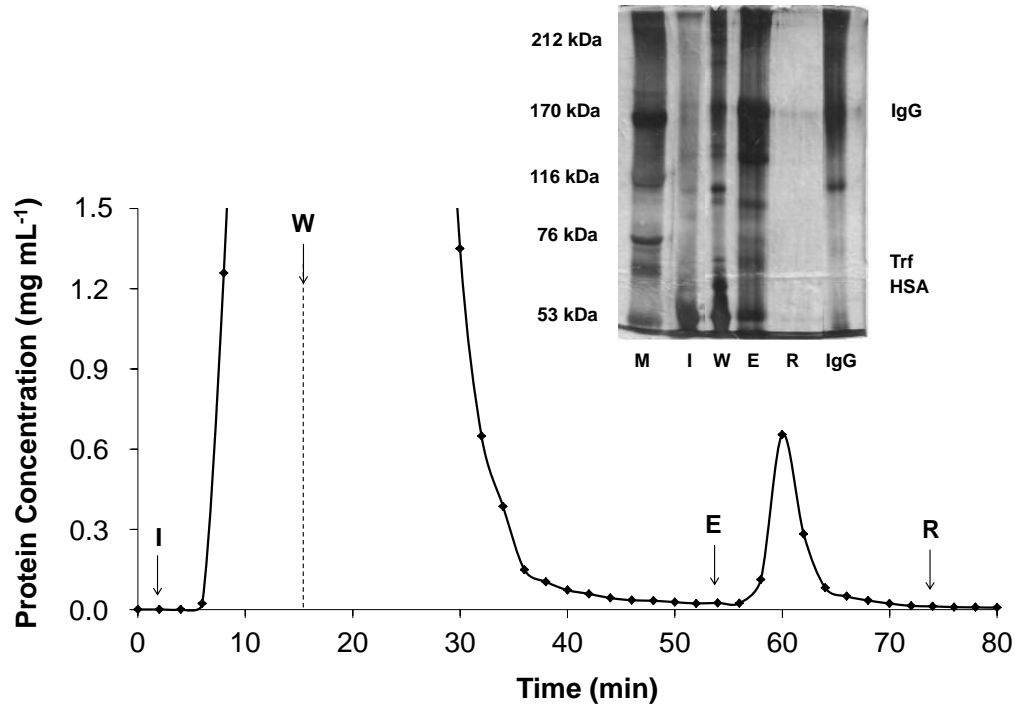


Figure 3.6. Chromatogram of the breakthrough curve of 15.0 mL of human serum diluted 10 times in 25 mmol/L sodium phosphate at pH 6.0 on Cibacron Blue F3GA immobilized on E-Ch/Al. Injection (I): 5,56 mg/mL of total protein; Washing (W): 25 mmol/L sodium phosphate buffer at pH 6.0; Elution (E): 25 mmol/L sodium phosphate buffer at pH 6.5 containing 1.0 mol/L of NaCl; Regeneration (R): 50 mmol/L of NaOH. In SDS-PAGE: M, molecular mass protein marker; I, initial solution; W, pool of washing fractions; E, pool of elution fractions; R, pool of regeneration fractions; and IgG, human IgG standard (Sigma).

Summary

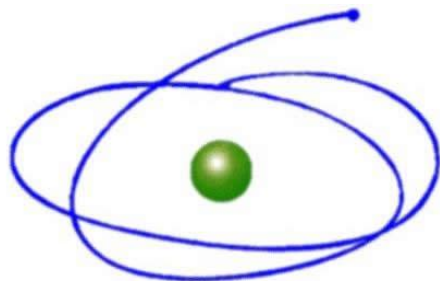
- Cibacron Blue F3GA-immobilized onto epoxide chitosan/alginate showed promising results for the adsorption of human IgG: it does not adsorb HSA significantly and retains IgG with relatively high capacity;
- Highest IgG uptakes are obtained at pH 6.0, at which the protein is mostly positively charged. Since sulphonated groups of Cibacron Blue are negatively charged at this pH, electrostatic interactions are likely to be the main binding mechanism;
- The dissociation constant – as estimated from Langmuir fits – is in the same order of magnitude as those presented in the literature for pseudo-bioaffinity ligands (10^{-6} mol/L).
- Non-optimized fixed bed runs give recoveries upon elution higher than 50% with good IgG selectivity

The team



Acknowledgements

- Prof. Enrique Rodríguez-Castellon
(Universidad de Málaga, Spain)
- Dr. Karim Sapag, Deicy Barrera and Johny Villaroel
(UNSL, Argentina)
- Dr. Igor Bresolin
(Universidade Federal de São Paulo, Brasil)



C A P E S

Coordenação de Aperfeiçoamento de Pessoal de Nível Superior



Special thanks



"Meeting Giorgio was like opening your first bottle of champagne; knowing him was like drinking it"

Eddy Tysoe, paraphrasing Winston Churchill